

Predicting extragalactic distance errors using Bayesian inference in multi-measurement catalogs

Germán Chaparro-Molano,^{1*} Juan Carlos Cuervo,² Oscar Alberto Restrepo Gaitán^{1,3}
 Sergio Torres Arzayús⁴

¹ Vicerrectoría de Investigación, Universidad ECCI, 111311 Bogotá, Colombia

² Department, Institution, Street Address, City Postal Code, Country

³ Radio Astronomy Instrumentation Group, Universidad de Chile, Santiago de Chile, Chile

⁴ Centro Internacional de Física, Bogotá, Colombia

Accepted XXX. Received YYY; in original form ZZZ

ABSTRACT

This is a simple template for authors to write new MNRAS papers. The abstract should briefly describe the aims, methods, and main results of the paper. It should be a single paragraph not more than 250 words (200 words for Letters). No references should appear in the abstract.

Key words: Galaxies: distances – keyword2 – keyword3

1 INTRODUCTION

Understanding the uncertainties in redshift-independent extragalactic distance measurements is absolutely necessary before reporting statistically sound conclusions regarding the structure of the local universe (Nasonova & Karachentsev 2011; Courtois et al. 2012; Ma et al. 2013; Springob et al. 2014; Sorce et al. 2014; Said et al. 2016; Kourkchi & Tully 2017), large scale structure (McClure & Dyer 2007; Roman & Trujillo 2017; Javanmardi & Kroupa 2017; Torres & Cuervo 2018; Jesus et al. 2018), and events like transient gravitational wave detections (White et al. 2011). Hubble constant estimations have been using increasingly sophisticated statistical tools for primary distance determination methods, such as SNIa (Barris & Tonry 2004; Rubin et al. 2015; Dhawan et al. 2018), Cepheids Humphreys et al. (2013) or both (Riess et al. 2016). Although most estimates of the Hubble constant use Cepheid calibration for calibrating secondary methods (Tully & Pierce 2000; Freedman et al. 2001; Freedman & Madore 2010), Mould & Sakai (2008) have explored changes in Hubble constant estimation using the Tully-Fisher relation (TF) relation without Cepheid calibration. Secondary methods for extragalactic distance determination like the TF relation, or the Fundamental Plane (FP) have recently become more precise thanks to increasing volumes of data from surveys like 6dF (Springob et al. 2014) and 2MASS (Jarrett et al. 2000; Springob et al. 2007) together with Spitzer data (Sorce et al. 2013), along with improved statistical methods (Obreschkow & Meyer 2013).

As of 2018, three multi-measurement catalogs including a substantial amount of redshift-independent extragalactic distance measurements have been released: HyperLEDA (Makarov et al. 2014), NED-D (Mazzarella & Team 2007; Steer et al. 2017), and Cosmicflows-3 (Tully et al. 2016). HyperLEDA includes a homogenized catalog for extragalactic distances in the nearby universe, with 12866 distance measurements for 518 galaxies to date. NED-D is the NASA/IPAC Extragalactic Distance catalog of Redshift-Independent Distances, which compiles 319690 distance measurements for 182170 galaxies, for which ~ 1800 galaxies ($\sim 1\%$) have more than 13 distance measurements, and 180 galaxies ($\sim 0.1\%$) have distance measurements using more than 6 different methods. Cosmicflows-3 is the most up-to-date catalog, which reports distance measurements for 10616 galaxies for up to four distance determination methods, and calibrated with supernova luminosities. However, unlike HyperLEDA or NED-D, Cosmicflows-3 only reports the latest distance measurement for each method. In HyperLEDA, NED-D and Cosmicflows-3 errors are reported as one standard deviation from the reported distance modulus. Treatment of errors for combining distance moduli across methods or across measurements is suggested by Mazzarella & Team (2007) and Tully et al. (2016) to be based on weighted estimates such as the uncertainty of the weighted mean, albeit with caution due to the heterogeneous origin of the compiled data. In the case of NED-D, this is complicated by the fact that many errors are not reported or are reported as zero. In fact, the TF relation method has the largest number of galaxies with non-reported distance modulus errors (818 to date). Even though extragalactic distances measured using the TF relation were originally reported to have a relative error

* E-mail: gchaparrom@ecci.edu.co

in distance modulus of $10 - 20\%$ (Tully & Fisher 1977), we consider that this conservative estimate can be improved upon by using a predictive model based on the distance error of galaxies that use the same distance determination method. This requires a robust estimation of the variance of extragalactic distances based on the available data.

For many galaxies in all three catalogs, the random error for each distance modulus measurement ϵ_i (for $i = 1, \dots, N$, for N distance measurements per galaxy) is not representative of the scatter across measurements, even when considering the same method for determining distances. In addition, distance modulus distributions for each measurement (which are assumed to be Gaussian) are transformed to log-normal distributions in metric distance space. We improve upon previous methods by robustly estimating the underlying variance across measurements and distance determination methods for the three catalogs by bootstrap sampling the posterior distribution of each extragalactic distance (Chaparro Molano et al. 2018). We compare our results to other more commonly used frequentist methods, such as the weighted estimates mentioned above. Furthermore, we build a predictive Bayesian model for the 818 galaxies in the NED-D catalog whose distances were measured using the TF relation but have non-reported errors, by performing posterior predictive checks using a discrepancy measure and a Bayesian “p-value” (Gelman et al. 1996).

Here go the sections.

2 POSTERIOR DISTRIBUTION FOR EXTRAGALACTIC DISTANCES

As mentioned in the Introduction, the best approach to consider the effects of random and scattering errors in catalog-wide, multi-method distance analyses is to perform a robust estimation of the variance of the posterior distribution of each extragalactic distance. The posterior distribution of the distance to a given galaxy can be obtained by drawing distance modulus bootstrap samples from $P(\mu)$, which is the unweighted mixture of normal distributions corresponding to each distance modulus measurement μ_i ,

$$\mu \sim \sum_i^N \mathcal{N}(\mu_i, \epsilon_i^2),$$

and then converting to metric distance,

$$D = 10^{\frac{\mu}{5} + 1}.$$

Therefore,

$$D_G \sim \sum_i^N \text{lognormal}(M_i, \sigma_{M_i}^2).$$

Here $M_i = \ln D_i$ and $\sigma_{M_i} = \epsilon_i \cdot \ln 10$.

However, this method is not very efficient for a standardized treatment of errors. It is more convenient to treat each extragalactic metric distance D_G as a normal random variable with a single-valued σ_D as a measure of the uncertainty in the estimation of an extragalactic distance,

$$D_G \sim \mathcal{N}(D, \sigma_D^2)$$

For this reason we compare four methods for estimating the D, σ_D pair. Two of these methods (H, M) use robust measures of the posterior distribution of each extragalactic distance, and the other two (P, Q) use measures based on propagation of errors.

2.1 Estimating the variance of $P(D_G)$

Method H takes D as the median of the posterior and σ_D as the half-distance (H) between the 84th and 16th percentiles of the posterior. Method M takes D as the median of the posterior and σ_D as the median absolute deviation (MAD) of the posterior. Method P consists on calculating D from the weighted mean distance modulus $\bar{\mu}^*$ with weights $w_i = \epsilon_i^{-2}$. σ_D is calculated by propagation (P) of measurement errors i.e. from the uncertainty of the weighted mean (Tully et al. 2016),

$$\sigma_D^P = 0.461 \bar{D}^* \left(\sum_i^N w_i \right)^{-1/2}, \quad (1)$$

Method P does not take into account the scatter in distance measurements for single galaxies, which is why method Q calculates D same as method P, but σ_D is calculated as the sum in quadrature (Q) of the propagated uncertainty of the weighted mean and the propagated unbiased weighted sample variance σ_D^* :

$$\sigma_D^Q = \left[\left(\sigma_D^P \right)^2 + \left(\sigma_D^* \right)^2 \right]^{1/2}. \quad (2)$$

Here σ_D^* is calculated as (Brugger 1969),

$$\sigma_D^* = 0.461 \bar{D}^* \sqrt{\frac{N}{N-1.5} \frac{\sum_i^N w_i (\mu_i - \bar{\mu}^*)^2}{\sum_i^N w_i}}. \quad (3)$$

If the non-robust P and Q methods are representative of the variance of the posterior, they should yield similar results as the H method. Next section shows that this is not the case.

2.2 Comparison of variance estimation methods

Without loss of generality, we will focus on galaxies whose distances have been measured using the Tully-Fisher method in the NED-D catalog because it is the method with the most non-reported errors in the database. From here on, when we mention distance measurements in the NED-D catalog, we will be excluding from our analysis measurements that require the target redshift to calculate the distance, as indicated in the `redshift (z)` field.

Even though our analysis for error estimation can be used to combine distance measurements using different methods for single galaxies, we think that it is more meaningful to separate the analysis by method. A full discussion of our error estimation method applied to multi-method measurements in the HyperLEDA, NED-D and Cosmicflows-3 is given in the appendix.

Fig. 1 shows that the center and variance of the posterior distribution of each extragalactic distance is best explained using the H method, whereas the less robust P and Q methods under-predict the variance for galaxies

in the whole distance range. The M method also under-predicts the variance, but being a robust method, it is not as sensitive to outliers as the methods P and Q, as seen in the case of NGC 1558 in Fig. 1. For the more symmetrical posterior distribution of UGC 12792, the M and Q methods predict the same center and variance.

Distance errors grow linearly with distance, as seen in Fig. 2. This means that there is a strong systematic component in the variance of $P(D_G)$. Furthermore, the quadrature (Q) and propagation (P) methods underpredict distance errors for most galaxies in the sample. Fig. 3 shows that method Q underpredicts distance errors with respect to the median absolute deviation method (M), which also shows a tighter linear correlation due to its robustness.

Given that each σ_D calculated using the H and M methods is obtained from many realizations from the posterior distribution of extragalactic distances, it is also possible to calculate its variance as the half-distance between the 84th and 16th percentile of bootstrap σ_D realizations. Fig. 4 shows that the variance of the estimated error is proportional to the error for the H and M methods. This will be relevant in Section 3 when we construct a predictive model for non-reported errors.

3 PREDICTIVE BAYESIAN MODELS FOR TF MISSING ERRORS

As seen in Figs. 2 and 3, TF distance errors estimated using the robust methods H and M grow in a roughly linear fashion with distance, but are randomly distributed around this trend line. For this reason we try out several Bayesian models in order to be able to predict missing distance errors. For this, we use the `emcee` affine invariant Markov Chain Monte Carlo (MCMC) ensemble sampler (Foreman-Mackey et al. 2013). Recently, `emcee` has been proved to be useful in obtaining probabilistic estimations for photometric redshifts Speagle & Eisenstein (2017a,b). Since we want to be able to predict non-reported errors, our model selection is based on posterior predictive checks, i.e. we rely on models that can create synthetic datasets similar to the original dataset (Gelman et al. 1996). This allows us to reproduce the original variance of the error (Fig. 4). Many Bayesian analyses often do not use posterior predictive checks, like in the work of Zhang & Shields (2018) and Jesus et al. (2018), where they used `emcee` for posterior sampling, and using Bayesian and Akaike Information Criteria along with Bayes factors for model assessment, but without attempting to reproduce the original variance of the data. This is also the case in other Bayesian tools like Linmix (Kelly 2007), which is widely used in astronomy for approximating unobserved data.

First we assume that for any galaxy j the distance error σ_{Dj} is a random normal variable, with variance $\sigma_{\sigma j}$ and mean $\hat{\sigma}_{Dj}$,

$$P(\sigma_{Dj}|\hat{\sigma}_{Dj}, \sigma_{\sigma j}) = \mathcal{N}(\hat{\sigma}_{Dj}, \sigma_{\sigma j}^2). \quad (4)$$

Our likelihood function is the joint probability that each of the $\sigma_D = \{\sigma_{Dj}\}$ in the original dataset of m galaxies is

generated by the above probability,

$$P(\sigma_D|\hat{\sigma}_D, \sigma_\sigma) = \prod_j^m P(\sigma_{Dj}|\hat{\sigma}_{Dj}, \sigma_{\sigma j}) \quad (5)$$

We want to test the hypothesis mentioned above that all errors and their variances ($\hat{\sigma}_D = \{\hat{\sigma}_{Dj}\}$, $\sigma_\sigma = \{\sigma_{\sigma j}\}$) can be estimated from a single model depending on the extragalactic distances $D_G = \{D_{Gj}\}$ and a set of distance-independent parameters $\boldsymbol{\theta}$. Thus the likelihood can be expressed as,

$$P(\sigma_D|D_G, \boldsymbol{\theta}) = \prod_j^m P(\sigma_{Dj}|D_{Gj}, \boldsymbol{\theta}).$$

Following Bayes' theorem we can compute the posterior probability up to a constant,

$$P(\boldsymbol{\theta}|D_G, \sigma_D) \propto P(\boldsymbol{\theta})P(\sigma_D|D_G, \boldsymbol{\theta}). \quad (6)$$

Due to the simplicity of the models used here, we will only use conservative (flat) priors. From our analysis of Fig. 4, all our models take $\sigma_\sigma = f\hat{\sigma}_D$. This error variance scale factor f is therefore one of the parameters in $\boldsymbol{\theta}$. On the other hand, our models will differ by the proposed functional forms of $\hat{\sigma}_D(D_G, \boldsymbol{\theta})$.

We obtain a computationally credible sampling of the posterior probability by removing the burn-in steps of the random walk according to the autocorrelation time. We can then create synthetic datasets by drawing a parameter sample $\boldsymbol{\theta}_k$ from the posterior and using it to draw from the likelihood to create a new dataset, i.e. drawing new σ_{Dj} from the probability distribution for all galaxies in the original dataset using equation 4. We then assess the validity of the model by comparing synthetic data with the observed (i.e. original) data. This comparison is done by using a discrepancy measure $\mathcal{D}(\sigma_D|\boldsymbol{\theta}_k)$ between data and model-derived expected values for the same data $e = \{e_j(\boldsymbol{\theta}_k)\}$, where $\boldsymbol{\theta}_k$ is drawn from the posterior distribution and σ_D can be the observed errors or the model-generated synthetic errors. The discrepancy can be calculated using a statistic like χ^2 (De la Horra 2008; de la Horra & Teresa Rodriguez-Bernal 2012), but here we will work with the Freeman-Tukey discrepancy since it is weight independent (Bishop et al. 2007; Brooks et al. 2000),

$$\mathcal{D}(\sigma_D|\boldsymbol{\theta}_k) = \sum_j^m (\sqrt{\sigma_{Dj}} - \sqrt{e_j(\boldsymbol{\theta}_k)})^2$$

For each parameter draw k , it is possible to compare the simulated discrepancy with the observed discrepancy. If the model is representative of the data, then for many parameter draws, the simulated and observed discrepancies should be similar. We can then calculate a Bayesian “*p*-value” as the ratio of “draws when the observed discrepancies are larger than the synthetic discrepancies” to “total draws”. If this Bayesian *p*-value is too close to 0 or to 1 we can reject the model, otherwise we cannot reject the model, as it is generating synthetic data that is similar to the original data. This is better visualized using a discrepancy plot, where for each draw k , a synthetic discrepancy is paired with its corresponding observed discrepancy. If the discrepancy points are roughly equally distributed about the $\mathcal{D}_{\text{obs}} = \mathcal{D}_{\text{sym}}$ line, then we cannot reject the model. We expect that galaxies with the largest number of measurements are sampling more

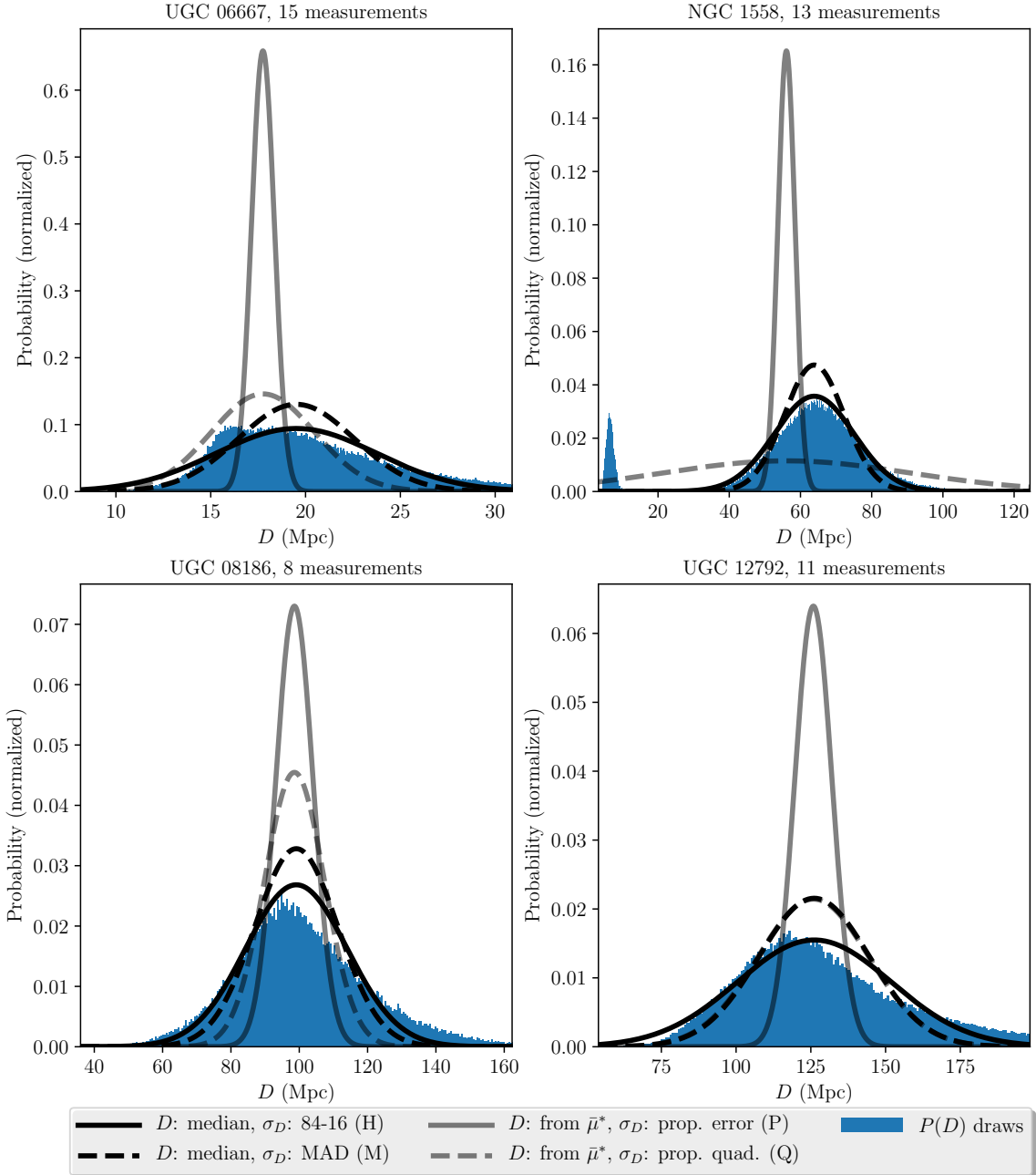


Figure 1. Comparison of extragalactic distance posterior distribution draws (10000 per measurement) and modeled distributions for UGC 06667, NGC 1558, UGC 08186, and UGC 12792 using the Tully-Fisher Method for distance determination in NED-D. The four methods used for approximating the posterior distribution (H, M, P, and Q) are described in the text.

completely the “true” distribution of the distance. Therefore we expect that if we set an increasing limit on the minimum number of measurements per galaxy on the dataset that goes in the model, the Bayesian p -value will improve.

3.1 Bayesian Quadrature Model

Our first model is based on the hypothesis that there are distinct systematic and random contributions to the distance measurement error, both of which are normally distributed.

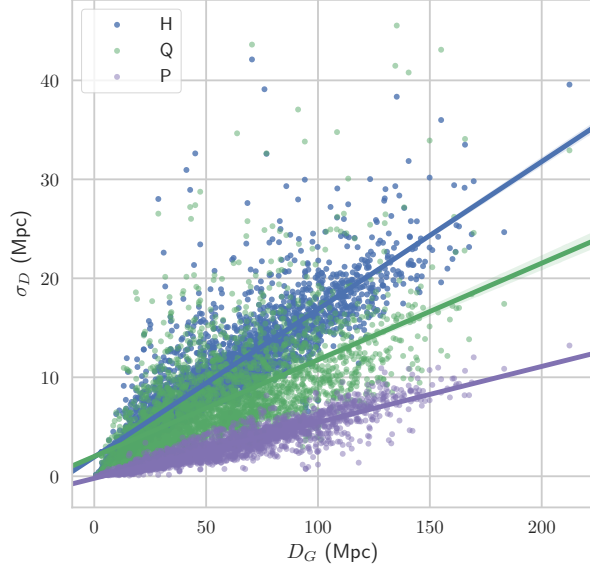


Figure 2. Median extragalactic distance vs. predicted extragalactic distance errors for galaxies with more than 5 TF distance measurements in NED-D according to the H, Q, P error models, showing a linear regression and confidence intervals computed using the `seaborn.regplot` Python function.

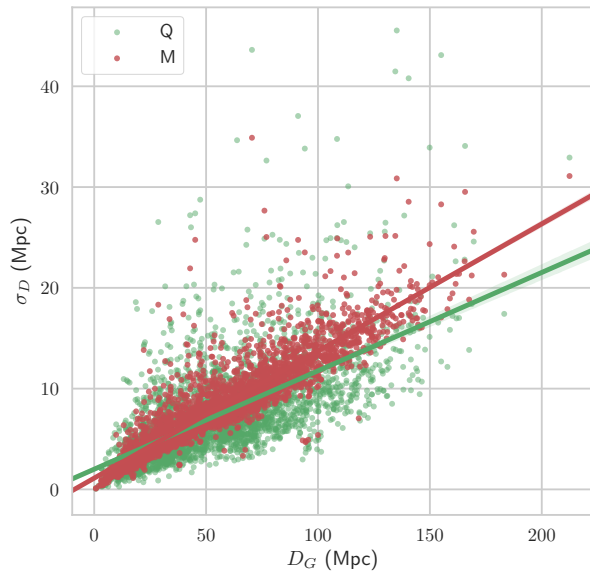


Figure 3. Median extragalactic distance vs. predicted extragalactic distance errors for galaxies with more than 5 TF distance measurements in NED-D according to the Q, M error models, showing a linear regression and confidence intervals computed using the `seaborn.regplot` Python function.

For this reason they are added in quadrature,

$$\sigma_D^2 = \sigma_s^2 + \sigma_r^2 . \quad (7)$$

Here σ_r is a random (constant) error and the systematic error is modeled allowing for scale factor (s) and zero setting (a) errors, i.e. $\sigma_s = sD + a$, as Fig. 2 suggests. We set our

prior to be symmetrical around $\sigma_r = 0$ in order to under-

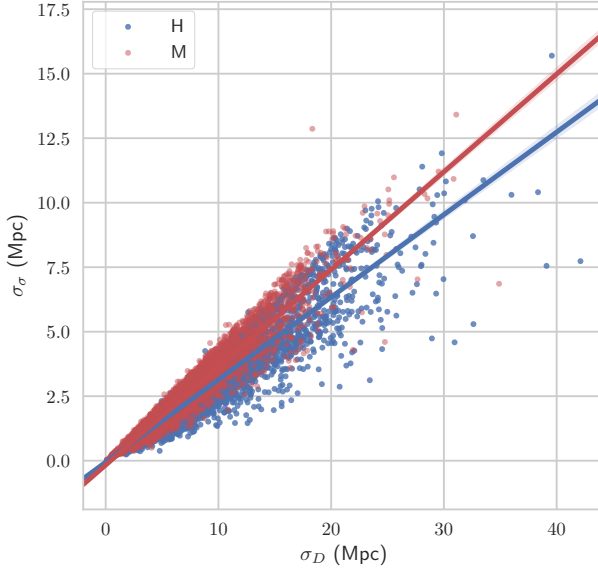


Figure 4. Predicted extragalactic distance errors vs. variance of the error as determined by the H and M methods, showing a linear regression and confidence intervals computed using the `seaborn.regplot` Python function.

stand its degeneracy, so

$$P(s, a, \sigma_r) = \begin{cases} 1, & \text{if } 0 < s < 1 \text{ and} \\ & 0 < a < 10 \text{ Mpc and} \\ & -10 < \sigma_r < 10 \text{ Mpc and} \\ & 0 < f < 1 \\ 0, & \text{otherwise.} \end{cases} \quad (8)$$

We now use `emcee` to sample the posterior over the parameter set $\boldsymbol{\theta} = (s, \sigma_r, f, a)$ using 100 walkers and 20000 steps ($t_{\text{autocorr}} \lesssim 90$ steps). According to the discrepancy plot in Fig. 5, this model is able to replicate method H errors for the 29 galaxies with $N > 25$ measurements (812 measurements in total). The corner plot showing the posterior sampling made by `emcee` is shown in Fig. 6, which shows that the systematic scale factor error is $s = 0.24^{+0.03}_{-0.03}$, the random error component is $\sigma_r = -0.004^{+1.294}_{-1.296}$ Mpc, the error variance scale factor is $f = 0.24^{+0.04}_{-0.03}$, and the zero offset systematic error is $a = 0.43^{+0.56}_{-0.34}$ Mpc. From the large variance in the marginalized posterior distribution for σ_r and a , we see that there is a significant degeneracy between those parameters. However, it should be noted that the marginalized posterior distribution of σ_r is symmetric around zero (because of its own degeneracy), while the distribution of a can only take positive values. The working distance range and overall fitting of this model is shown in Fig. 7, where the method H errors corresponding to galaxies with more than 25 TF distance measurements are plotted along the expected values $e = \{e_j(\boldsymbol{\theta}_k)\}$ for parameter sets $\boldsymbol{\theta}_k$ drawn from the posterior probability distribution. Now we sample the posterior distribution for the Bayesian quadrature model with method M errors using `emcee` with 100 walkers and 20000 steps s ($t_{\text{autocorr}} \lesssim 50$ steps). The discrepancy plot for method M errors in Fig. 8 shows that the quadrature model also replicates method M errors, but for the 727 galaxies with

more than 13 measurements (12947 measurements in total). Fig. 9, shows that $s = 0.142^{+0.003}_{-0.003}$, $\sigma_r = 0.004^{+0.201}_{-0.201}$ Mpc, $f = 0.228^{+0.007}_{-0.006}$, and $a = 0.52^{+0.06}_{-0.06}$ Mpc. The random error is so low that the model draws are almost indistinguishable from straight lines in Fig 10. Additionally, and just as for the quadrature model for H errors above, the symmetry of the marginalized posterior distribution of σ_r leads us to set this parameter to zero in our next model in order to improve numerical stability.

3.2 Bayesian Linear Model

In Section 3.1 above we conclude that we can ignore the random error component in equation 7 in order to work with a simpler, numerically stable, linear model that only considers a systematic error with scale factor and zero setting error components,

$$\sigma_D = \sigma_s = sD + a. \quad (9)$$

We also update our prior considering that the quadratic model yielded lower values for the zero setting error a than previously considered in equation 8,

$$P(s, a, \sigma_r) = \begin{cases} 1, & \text{if } 0 < s < 1 \text{ and} \\ & 0 < a < 2 \text{ Mpc and} \\ & 0 < f < 1 \\ 0, & \text{otherwise.} \end{cases} \quad (10)$$

We use `emcee` to sample the posterior over $\boldsymbol{\theta} = (s, a, f)$ using 100 walkers and 10000 steps ($t_{\text{autocorr}} < 50$ steps) for the linear Bayesian model applied to H errors. The discrepancy plot (Fig. 11) shows a significant improvement over the quadratic model, as it shows an acceptable Bayesian p -value for the 473 galaxies with $N > 15$ measurements (9259 in total), whereas the quadratic model replicated errors only for

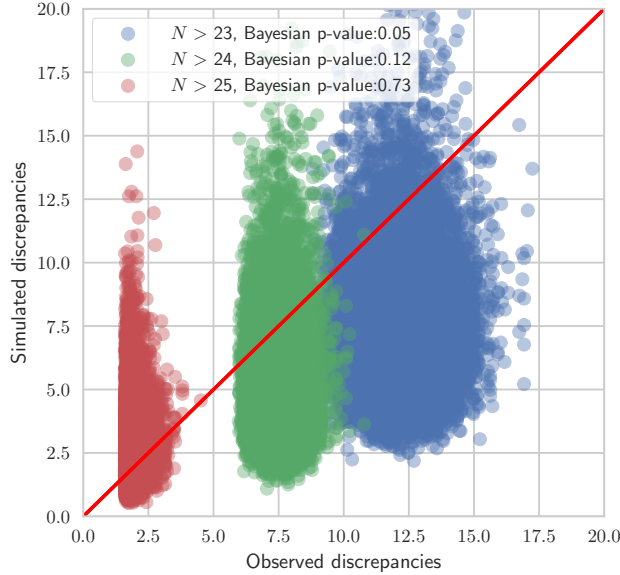


Figure 5. Discrepancy plot for the Bayesian quadrature model (equation 7) based on errors estimated using method H.

Table 1. This is an example table. Captions appear above each table. Remember to define the quantities, symbols and units used.

A	B	C	D
1	2	3	4
2	4	6	8
3	5	7	9

galaxies with $N > 25$ measurements. Fig. 12, shows that for the linear Bayesian model using H errors for galaxies with more than 15 measurements, $s = 0.200_{-0.006}^{+0.006}$, $a = 0.76_{-0.12}^{+0.13}$ Mpc, and $f = 0.256_{-0.009}^{+0.009}$. We sample the posterior for the linear model applied to M errors using emcee with 100 walkers and 10000 steps ($t_{\text{autocorr}} < 50$ steps). Fig. 14 shows the discrepancy plot, which does not show a significant improvement of the linear over the quadratic model for M errors, as it also works for galaxies with $N > 13$ measurements. This happens because the sampling of the posterior for the quadratic model (Fig. 9) does not show a degeneracy between σ_r and a , and also because the marginalized posterior distribution for σ_r is a near-zero distribution with a variance of 0.2 Mpc. The parameters according the the linear model and data are $s = 0.142_{-0.003}^{+0.003}$, $a = 0.53_{-0.06}^{+0.06}$ Mpc, and $f = 0.228_{-0.006}^{+0.006}$, as shown in Fig. 15. Figs. ?? and ?? show

3.3 Predictions for missing errors

Gelman (2003) and Chambert, Rotella & Higgs (Chambert et al.) and for using posterior predictive checks for inference and prediction

4 CONCLUSIONS

Discrepancy plots should be more widely used

ACKNOWLEDGEMENTS

The authors would like to thank O. L. Ramírez-Suárez and J. E. Forero-Romero for their valuable input during the early stages of this work. This research has made use of the NASA/IPAC Extragalactic Database (NED), which is operated by the Jet Propulsion Laboratory, California Institute of Technology, under contract with the National Aeronautics and Space Administration.

REFERENCES

- Barris B., Tonry J., 2004, *ASTROPHYSICAL JOURNAL*, 613, L21
- Bishop Y. M. M., et al., 2007, *Discrete Multivariate Analysis: Theory and Practice*. Springer
- Brooks S. P., Catchpole E. A., Morgan B. J. T., 2000, *Statistical Science*, 15, 357
- Brugger R. M., 1969, *The American Statistician*, 23, 32
- Chambert T., Rotella J. J., Higgs M. D., , *Ecology and Evolution*, 4, 1389
- Chaparro Molano G., Restrepo Gaitán O. A., Cuervo Marulanda J. C., Torres Arzayus S. A., 2018, in Revista Mexicana de Astronomía y Astrofísica Conference Series. pp 63–63
- Courtois H. M., Hoffman Y., Tully R. B., Gottloeber S., 2012, *ASTROPHYSICAL JOURNAL*, 744
- De la Horra J., 2008, *COMMUNICATIONS IN STATISTICS-THEORY AND METHODS*, 37, 1412
- Dhawan S., Jha S. W., Leibundgut B., 2018, *ASTRONOMY & ASTROPHYSICS*, 609
- Foreman-Mackey D., Hogg D. W., Lang D., Goodman J., 2013,

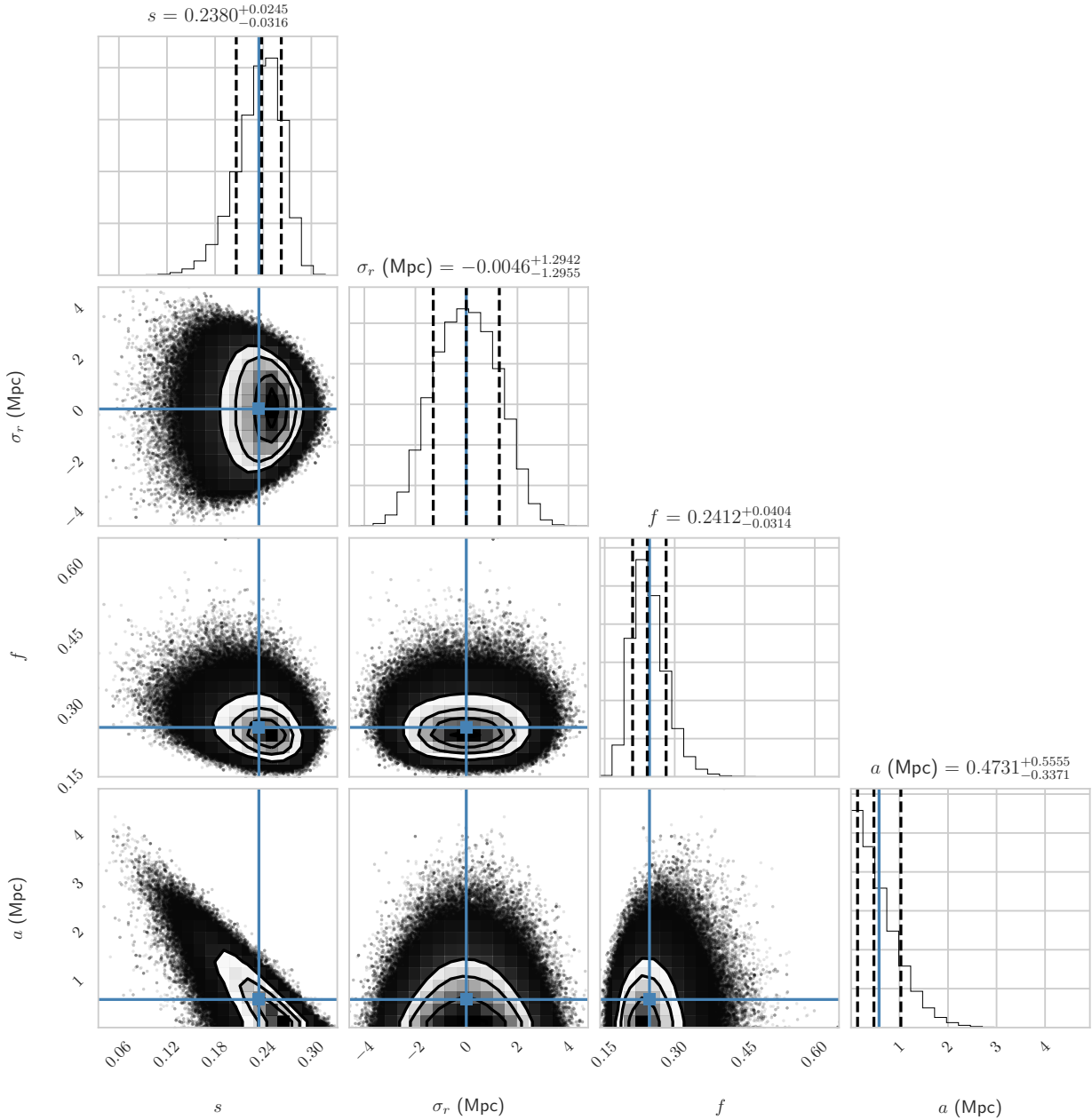


Figure 6. Corner plot showing the `emcee` sampling of the posterior probability distribution (equation 6) for the quadrature Bayesian model parameters $\theta = (s, \sigma_r, f, a)$ based on errors estimated using method H for galaxies with more than 25 TF distance measurements. The dashed lines indicate the 16th, 50th, and 84th percentile of the marginalized distribution of each parameter (shown at the top of each column), and the blue solid lines indicate the mean. This plot was made using the `corner` Python module.

- PUBLICATIONS OF THE ASTRONOMICAL SOCIETY OF THE PACIFIC, 125, 306
- Freedman W. L., Madore B. F., 2010, in Blandford R., Faber S., van Dishoeck E., Kormendy J., eds, Annual Review of Astronomy and Astrophysics, Vol. 48, ANNUAL REVIEW OF ASTROPHYSICS AND ASTROPHYSICS, VOL 48, pp 673–710, doi:10.1146/annurev-astro-082708-101829
- Freedman W. L., et al., 2001, The Astrophysical Journal, 553, 47
- Gelman A., 2003, Internat. Statist. Rev., 71, 369
- Gelman A., Li Meng X., Stern H., 1996, Statistica Sinica, 6, 733
- Humphreys E. M. L., Reid M. J., Moran J. M., Greenhill L. J., Argon A. L., 2013, ASTROPHYSICAL JOURNAL, 775

- Jarrett T. H., Chester T., Cutri R., Schneider S., Skrutskie M., Huchra J. P., 2000, The Astronomical Journal, 119, 2498
- Javanmardi B., Kroupa P., 2017, ASTRONOMY & ASTROPHYSICS, 597
- Jesus J. F., Gregório T. M., Andrade-Oliveira F., Valentim R., Matos C. A. O., 2018, MNRAS,
- Kelly B. C., 2007, ASTROPHYSICAL JOURNAL, 665, 1489
- Kourkchi E., Tully R. B., 2017, ASTROPHYSICAL JOURNAL, 843
- Ma Y.-Z., Taylor J. E., Scott D., 2013, MONTHLY NOTICES OF THE ROYAL ASTRONOMICAL SOCIETY, 436, 2029
- Makarov D., Prugniel P., Terekhova N., Courtois H., Vauglin I.,

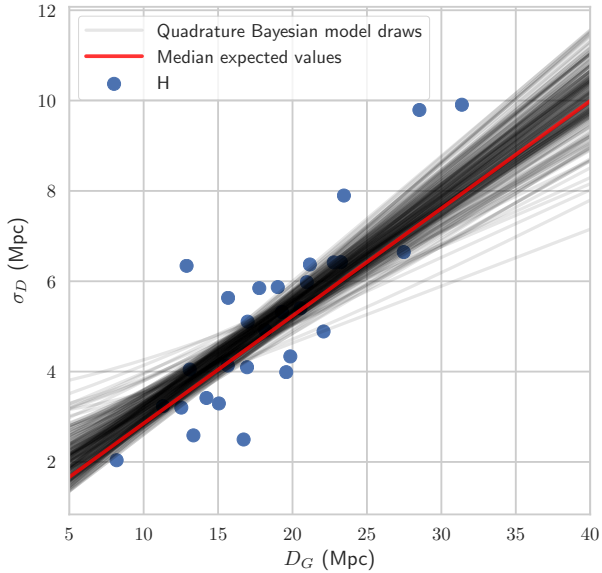


Figure 7. Projection of parameter set samples from the posterior probability distribution of the Bayesian quadrature model onto the D_G vs. σ_D scatter plot for errors estimated using method H for galaxies with more than 25 TF distance measurements.

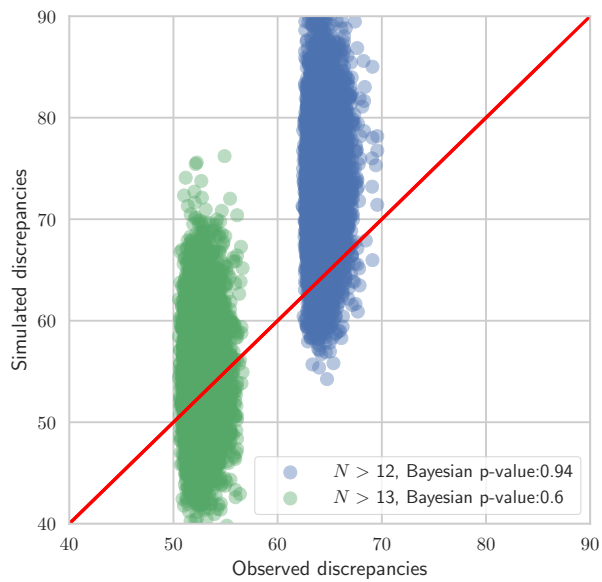


Figure 8. Discrepancy plot for the Bayesian quadrature model (equation 7) based on errors estimated using method M.

- 2014, *ASTRONOMY & ASTROPHYSICS*, 570
 Mazzarella J. M., Team N., 2007, in Shaw R., Hill F., Bell D., eds, ASTRONOMICAL SOCIETY OF THE PACIFIC CONFERENCE SERIES Vol. 376, ASTRONOMICAL DATA ANALYSIS SOFTWARE AND SYSTEMS XVI. pp 153–162
 McClure M. L., Dyer C. C., 2007, *NEW ASTRONOMY*, 12, 533
 Mould J., Sakai S., 2008, *ASTROPHYSICAL JOURNAL LETTERS*, 686, L75
 Nasonova O. G., Karachentsev I. D., 2011, *ASTROPHYSICS*, 54,

- 1
 Obreschkow D., Meyer M., 2013, *ASTROPHYSICAL JOURNAL*, 777
 Riess A. G., et al., 2016, *The Astrophysical Journal*, 826, 56
 Roman J., Trujillo I., 2017, *MONTHLY NOTICES OF THE ROYAL ASTRONOMICAL SOCIETY*, 468, 703
 Rubin D., et al., 2015, *ASTROPHYSICAL JOURNAL*, 813
 Said K., Kraan-Korteweg R. C., Staveley-Smith L., Williams W. L., Jarrett T. H., Springob C. M., 2016, *MONTHLY NO-*

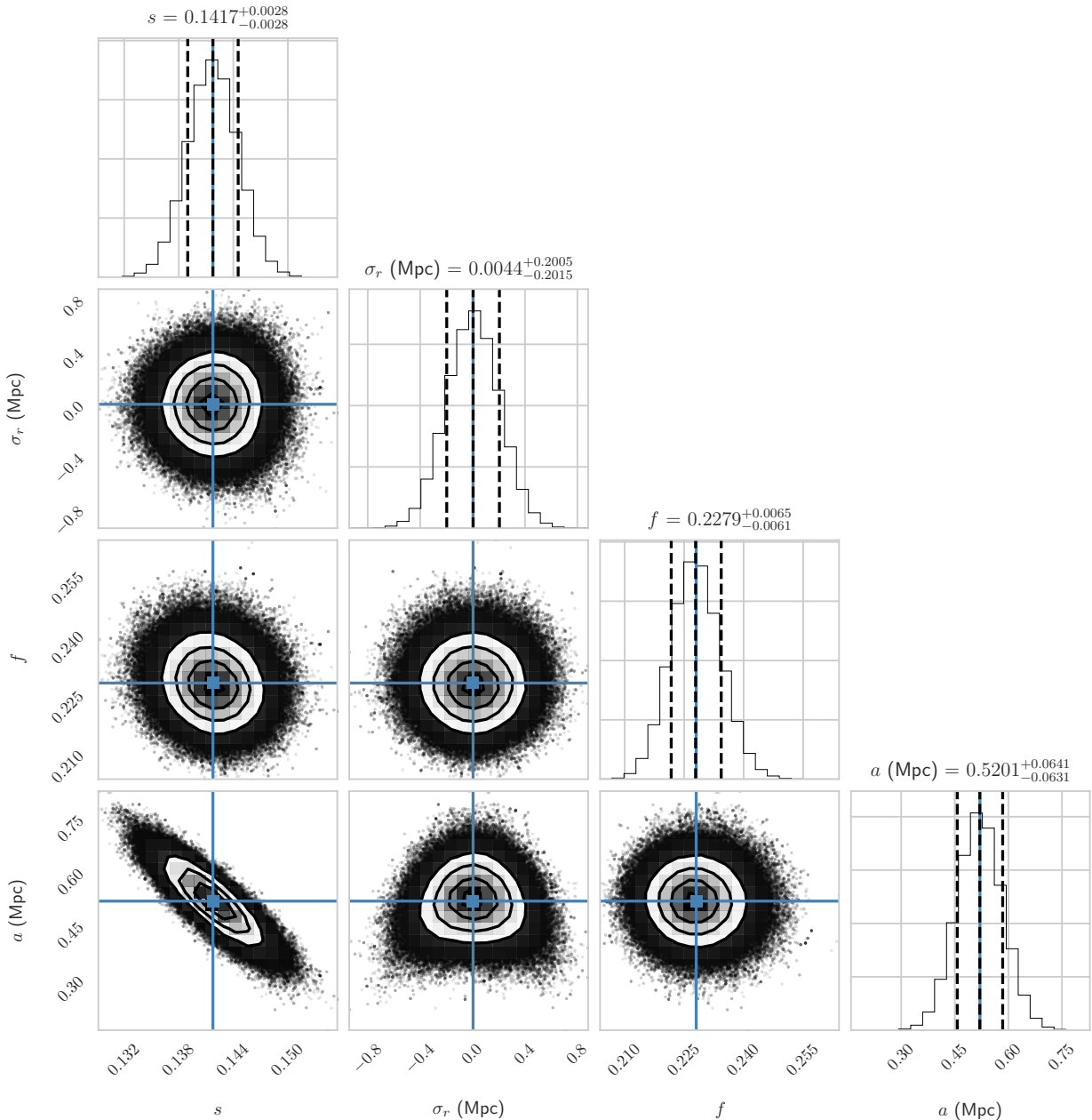


Figure 9. Corner plot showing the `emcee` sampling of the posterior probability distribution (equation 6) for the quadrature Bayesian model parameters $\theta = (s, \sigma_r, f, a)$ based on errors estimated using method M for galaxies with more than 13 TF distance measurements. The dashed lines indicate the 16th, 50th, and 84th percentile of the marginalized distribution of each parameter (shown at the top of each column), and the blue solid lines indicate the mean. This plot was made using the `corner` Python module.

- TICES OF THE ROYAL ASTRONOMICAL SOCIETY, 457, 2366
Sorce J. G., et al., 2013, The Astrophysical Journal, 765, 94
Sorce J. G., Courtois H. M., Gottlöber S., Hoffman Y., Tully R. B., 2014, *MONTHLY NOTICES OF THE ROYAL ASTRONOMICAL SOCIETY*, 437, 3586
Speagle J. S., Eisenstein D. J., 2017a, *MONTHLY NOTICES OF THE ROYAL ASTRONOMICAL SOCIETY*, 469, 1186
Speagle J. S., Eisenstein D. J., 2017b, *MONTHLY NOTICES OF THE ROYAL ASTRONOMICAL SOCIETY*, 469, 1205
Springob C. M., Masters K. L., Haynes M. P., Giovanelli R., Marinoni C., 2007, The Astrophysical Journal Supplement Series,

- 172, 599
Springob C. M., et al., 2014, *MONTHLY NOTICES OF THE ROYAL ASTRONOMICAL SOCIETY*, 445, 2677
Steer I., et al., 2017, *ASTRONOMICAL JOURNAL*, 153
Torres S., Cuervo J. C., 2018, *Tecciencia*, 24, 53
Tully R. B., Fisher J. R., 1977, *A&A*, 54, 661
Tully R. B., Pierce M. J., 2000, The Astrophysical Journal, 533, 744
Tully R. B., Courtois H. M., Sorce J. G., 2016, *ASTRONOMICAL JOURNAL*, 152
White D. J., Daw E. J., Dhillon V. S., 2011, *CLASSICAL AND QUANTUM GRAVITY*, 28

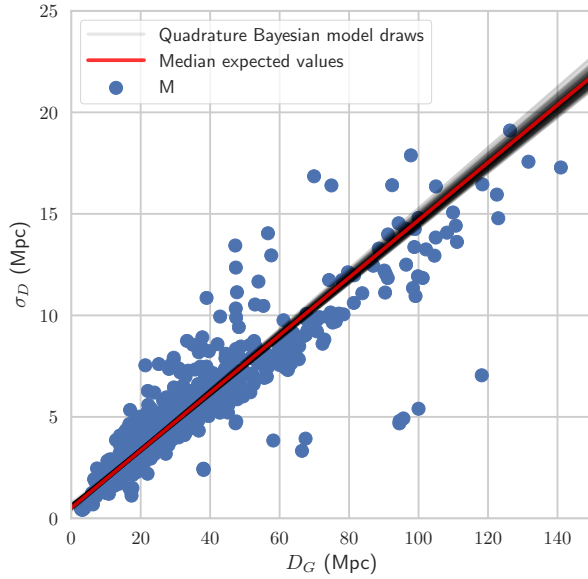


Figure 10. Projection of parameter set samples from the posterior probability distribution of the Bayesian quadrature model onto the D_G vs. σ_D scatter plot for errors estimated using method M for galaxies with more than 13 TF distance measurements.

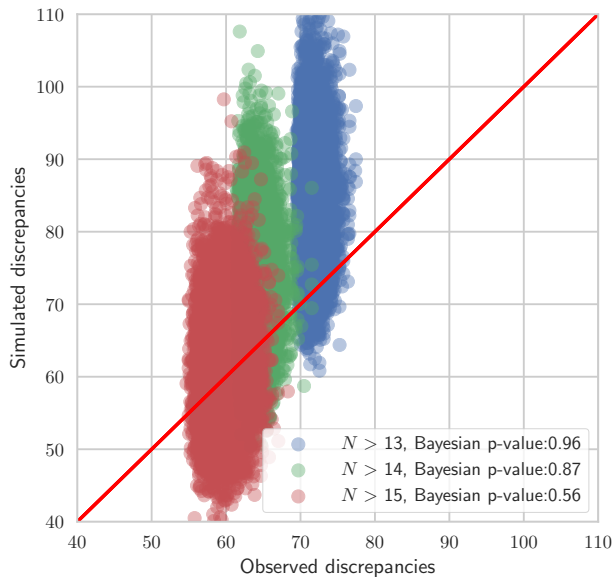


Figure 11. Discrepancy plot for the Bayesian linear model (equation 9) based on errors estimated using method H.

- Zhang J., Shields M. D., 2018, *MECHANICAL SYSTEMS AND SIGNAL PROCESSING*, 98, 465
de la Horra J., Teresa Rodriguez-Bernal M., 2012, *SORT-STATISTICS AND OPERATIONS RESEARCH TRANSACTIONS*, 36, 69

APPENDIX A: SOME EXTRA MATERIAL

Bootstrap H and M treatment for HyperLEDA, NED-D and Cosmicflows-3, along with plots (3 plots total). NED-D per-method error?

This paper has been typeset from a $\text{TeX}/\text{\LaTeX}$ file prepared by the author.

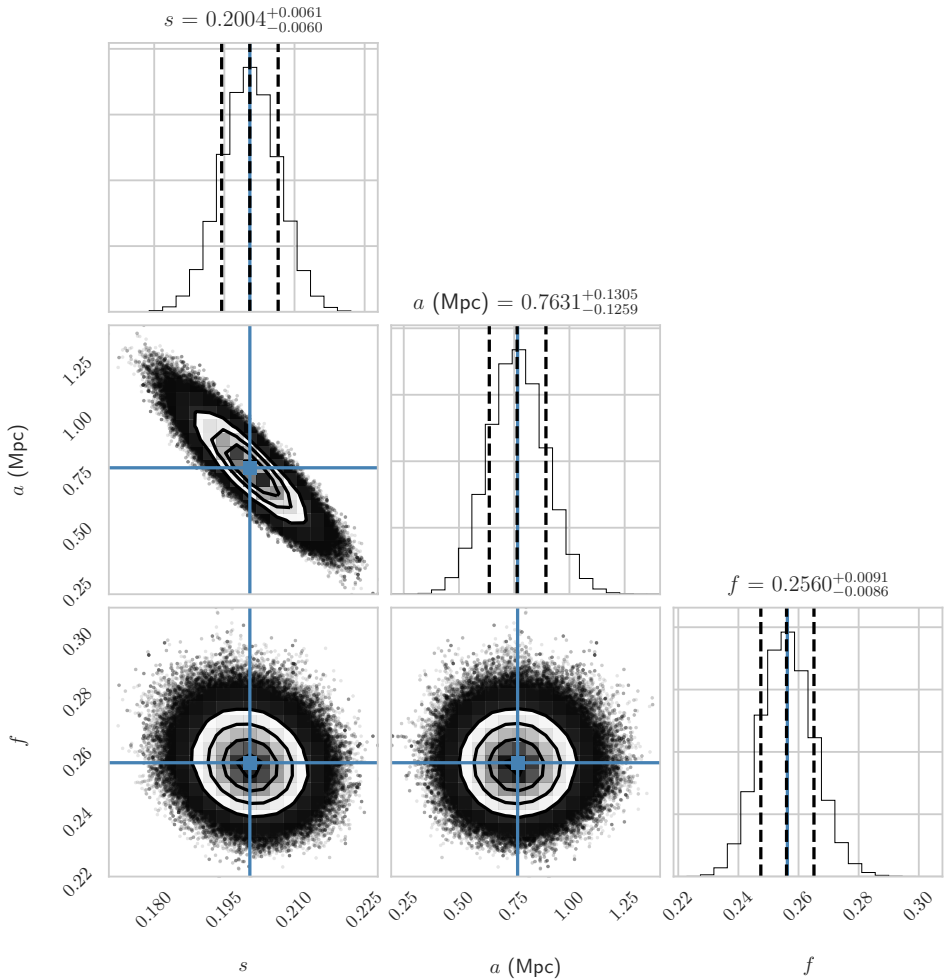


Figure 12. Corner plot showing the `emcee` sampling of the posterior probability distribution (equation 6) for the linear Bayesian model parameters $\boldsymbol{\theta} = (s, a, f)$ based on errors estimated using method H for galaxies with more than 15 TF distance measurements. The dashed lines indicate the 16th, 50th, and 84th percentile of the marginalized distribution of each parameter (shown at the top of each column), and the blue solid lines indicate the mean. This plot was made using the `corner` Python module.

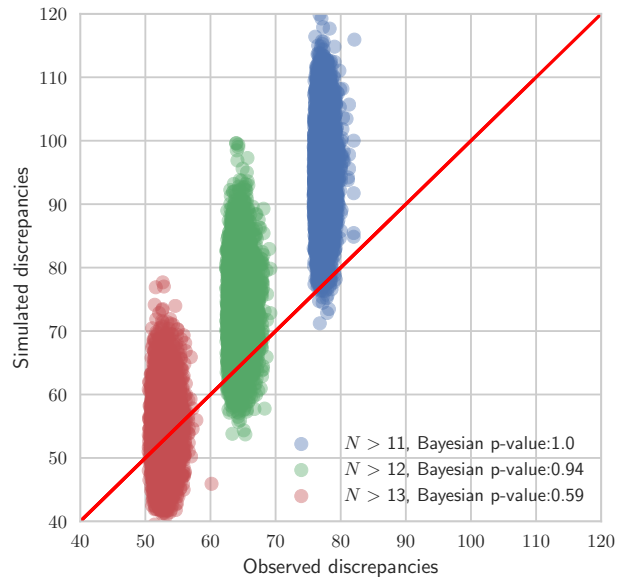


Figure 13. Discrepancy plot for the Bayesian linear model (equation 9) based on errors estimated using method M.

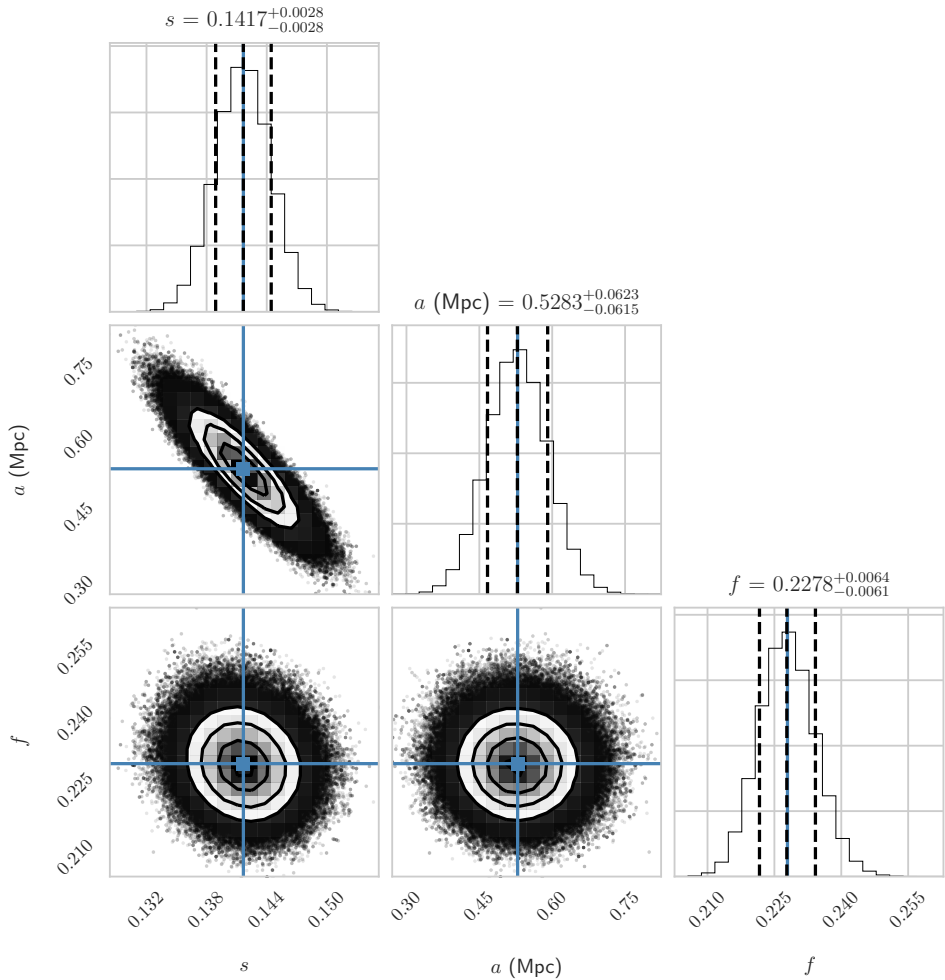


Figure 14. Corner plot showing the `emcee` sampling of the posterior probability distribution (equation 6) for the linear Bayesian model parameters $\boldsymbol{\theta} = (s, a, f)$ based on errors estimated using method M for galaxies with more than 13 TF distance measurements. The dashed lines indicate the 16th, 50th, and 84th percentile of the marginalized distribution of each parameter (shown at the top of each column), and the blue solid lines indicate the mean. This plot was made using the `corner` Python module.

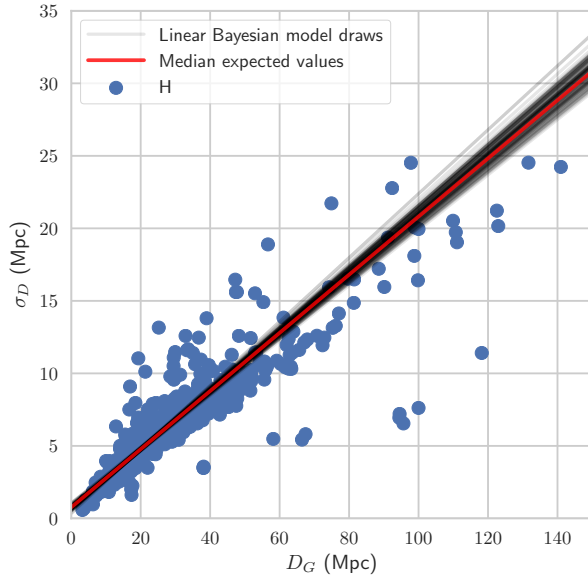


Figure 15. Projection of parameter set samples from the posterior probability distribution of the Bayesian linear model onto the D_G vs. σ_D scatter plot for errors estimated using method H for galaxies with more than 15 TF distance measurements.

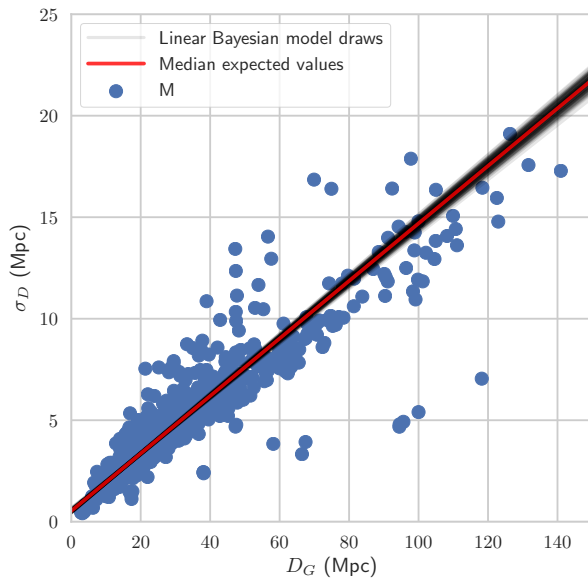


Figure 16. Projection of parameter set samples from the posterior probability distribution of the Bayesian linear model onto the D_G vs. σ_D scatter plot for errors estimated using method M for galaxies with more than 13 TF distance measurements.